Journal Home Page: https://sjes.univsul.edu.iq/

Research Article:

Two-way Slabs having Openings Strengthened with Heavy-Duty Metal Straps

Mohammed Ahmed Hassan [1,a,*]
Wrya Abdul faraj Abdullah[2,a]
[a] Department of Civil Engineering, College of Engineering, University of Sulaimani, Kurdistan Region, Iraq

Article Information

Article History:
Received: September 21st ,2025
Accepted : February 25th ,2026
Available online: April , 2025

Keywords:
Two-way slab
Opening ,Strengthening , Structural performance , Heavy-Duty Metal Strap.

About the Authors:
Corresponding author:
Mohammed Ahmed Hassan
E-mail Muhammed.hassan@univsul.edu.iq
Researcher Involved:
Dr. Wrya Abdul Faraj Abdullah
E-mail wrya.faraj@univsul.edu.iq

DOI https://doi.org/10.17656/sjes.10200

Abstract

Openings in slabs are commonly implemented to facilitate mechanical and electrical services; however, they considerably reduce stiffness, load-carrying capacity, and ductility, potentially changing failure modes. This study conducts an experimental analysis of twelve two-way normal reinforced concrete (RC) slabs, including one solid control slab, three unstrengthened slabs with openings at various locations (Middle, Corner, and Edge) in the specimens, and eight strengthened slabs utilizing Heavy-Duty Metal Straps (HDMS) which are thin steel strapping bands used externally as a strengthening system. The findings indicated that unstrengthened slabs with openings demonstrated considerable decreases in ultimate load capacity (up to 20% lower than the solid control) and flexural stiffness, with failure modes primarily transitioning to punching shear. The strengthening of corner openings restored the ultimate strength to levels similar to those of the solid control slab and increased stiffness by over 40%, in addition to improving ductility performance. The strengthening for middle openings resulted in partial recovery of stiffness and ultimate load, alongside significant enhancements in ductility. The performance of HDMS at edge openings was dependent on configuration; in the optimal arrangement, the technique nearly restored ultimate stiffness to the control level, while other configurations exhibited limited advantages.

1. Introduction

Structural engineers frequently face the challenge of facilitating access for utility services within existing reinforced concrete slabs. In numerous instances, openings are required in slabs at locations not accounted for during the structural design of a building. This necessity arises mostly from a sequence of alterations in functioning. There are instances where certain openings were incorporated during the design phase; nevertheless, alterations in functionality or purpose have resulted in a substantial increase in the loads imposed on the slabs [1]. ACI 318-19 [2] stipulates that openings in two-way slabs must be meticulously positioned and strengthened. Minor openings distant from column areas are permissible with basic reinforcement detailing; however, bigger openings or those near supports substantially diminish punched shear and flexural capability, necessitating additional reinforcement, framing, or redesign. Eurocode 2 [3] specifies that openings in slabs diminish both flexural and shear strength. Minor openings can be supported with localized reinforcement; however, larger openings, particularly those situated inside the punching shear zone, necessitate a reduction in the effective shear perimeter and may require supplementary reinforcement or framing. The code underscores the continuity of reinforcement at openings and meticulous consideration of shear transfer. The inclusion of openings in such slabs often results in excessive stresses that are harmful unless adequately evaluated and engineered [4]. Chand Dewangan et al. [5] and Nageswara Rao et al. [6], conducted numerical analyses of stress distribution surrounding cutouts to assess failure capacity. These openings not only

diminish the strength and rigidity of the slabs, but they also alter the original failure mode of the slab to different failure patterns [7] . The presence of the opening diminishes the volume of concrete that contributes to resisting shear forces and unbalanced moments, hence further decreasing the punching shear capacity of the slab-column connection. The slab-column connection is hence more susceptible to brittle punching shear failure [8]. Currently, the reconstruction of existing structures has become increasingly prevalent due to the structural and/or functional demands of users [9]. Such reconstruction process mostly contains introduction of openings in the slabs, so it is important to study various strengthening techniques for this purpose. Researchers tested different methods for strengthening especially for reinforced concrete slabs with openings and each obtained different results considering the controlling deflection, stiffness modification, and resistance to shear and flexure. Recent studies focused on the application of CFRP for the reinforcement of reinforced concrete constructions [10] and [11]. The application of FRP sheets for enhancing the flexural capacity of concrete slabs is effectively beneficial due to their superior strength and straightforward installation process. Reinforcement using FRP necessitates specialized craftsmanship in contrast to traditional steel strips or alternative strengthening methods. High tensile stress can be achieved in CFRP, provided that the load-bearing capacity of the component is not constrained by an early failure mode [12] and [13]. Mahlis et al. [14]conducted an experimental study on ten square reinforced concrete two-way beamed slabs, each measuring 1000 mm x 1000 mm with a thickness of 150 mm, the reinforcement was with 8 mm diameter steel bars spaced at 100 mm center-to-center intervals. The study found that a 300 mm square mid-span opening reduced the load-bearing capacity of slabs by 18.2% compared to slabs without openings. The addition of internal steel reinforcement surrounding the opening improved the load-carrying capacity by 15% to 51%, depending on the development length and arrangement of the reinforcing bars. The NSM approach and externally bonded CFRP laminates successfully reinstated the load-carrying capacity of the slab, particularly through the use of extended anchoring lengths for the reinforcement. The study found that the presence of openings significantly affects the structural performance of slabs, and that appropriate reinforcement techniques can improve their load-bearing capacity. Banu et al. [15]conducted a study on two series of reinforced concrete slabs to evaluate the effectiveness of Carbon Fibre Reinforced Polymer (CFRP) strips for reinforcement. The original series consisted of four unperforated slabs, whereas the subsequent series featured four slabs with a central opening. Each series contained one control slab that was unreinforced with CFRP strips and three slabs reinforced with CFRP in different configurations. The size of the slabs were 110 cm × 110 cm x 5 cm. The study demonstrated that utilizing CFRP strips for slab reinforcement provided significant advantages over traditional methods. The benefits included a minimal increase in permanent loads, resistance to corrosion, and the ability to customize the orientation of the FRP fibers to improve reinforcement in the required directions. The test setup and instrumentation enabled an assessment of the total stiffness and flexural capacity of the reinforced slabs in comparison to the control slabs. Elsayed [16] investigated the performance of reinforced concrete (RC) slabs augmented in flexural capacity by a mechanically bonded fiber-reinforced polymer (FRP) system. Two sets of comprehensive reinforced concrete slabs were assessed. The initial series consisted of five slabs without cut-outs, each measuring (2600 x 2600 x 120) mm, whereas the subsequent series had four slabs of the same dimensions, each with a central cut-out of (800 x 800) mm. The reinforced slabs demonstrated improved strength, stiffness, and ductility, marked by increased ductility indices and energy absorption due to the Mechanically Fastened system. Under load, bearing failure occurred in the FRP at the region of highest strain, leading to pseudo-ductile failure as the load was sequentially passed via the fasteners. The progressive bearing failure continued after the yielding of steel reinforcement, optimizing FRP utilization without delamination and resulting in a ductile failure mechanism. Heavy-duty metal straps (HDMS) are a well-known way to make reinforced concrete beams stronger. Their use has led to improvements in load resistance, flexural capacity, and crack control, making them a useful and cost-effective way to strengthen structures. This methodology, initially derived from packaging technology, has been evaluated for the reinforcement of various reinforced concrete components, including concrete cylinders, columns, beams (under both flexural and shear loads), lap-spliced elements, and joints, as well as in full-scale structures exposed to seismic simulations. Neupane et al.[17] stated that post-tensioned metal strapping (PTMS), a new active confinement method, can greatly improve the performance of concrete buildings. They stated that the axial load capacity can be increased by 80–120%, the ductility can be increased by up to 100%, the bond strength by 58%, and the bending moment capacity by 69–157%. This shows that these approaches are better than traditional strengthening methods. Imjai et al.[18] examined the post-tensioned metal strapping (PTMS) method, which employs metal straps tensioned with conventional steel strapping technique

to actively constrain reinforced concrete (RC) constructions. PTMS has demonstrated significant efficacy in augmenting the load-bearing capacity and ductility of these components, giving better resistance to stresses from compression, shear, flexure, and bond-splitting. Although this technique has been used for strengthening beams and columns, but still has not utilized it for strengthening slabs especially those having openings. The goal from this study is to show the strengthening technique using HDMS that is used for openings in the reinforced concrete two-way slabs and making a comparison between each configuration in accordance with the load-carrying capacity, stiffness enhancement, deflection control by demonstrating the results obtained in this study from the point of view of the effectiveness, economy and the ease of application with minimum suitable required time for the process.

2. Experimental program

2.1 Study Parameters

This study involved the casting of twelve two-way normal reinforced concrete slabs, which were subjected to incremental static loading for testing. All tested slabs had identical dimensions: a thickness of 100 mm, a width of 1200 mm, and a length of 1200 mm, while the center-to-center measurement from support to support is 1080 mm in each direction. The study employed a set of variables, including: the introduction of openings at various locations (Middle, Corner, and Edge) in the slabs to evaluate their influence on structural performance; the application of HDMS for reinforcement on the tension face of the slabs, along with an analysis of the effects of each configuration; and the integration of anchor bolts with metal straps to im-prove bond strength and reduce debonding, in order to assess the efficacy of the strengthening technique. The parameters and slab nomenclatures are provided in Table 1. The nomenclature of each slab consists of several symbols. For example, the first (S) symbols represent the element type which is slab, the second (S) letter represents slabs strengthened with metal straps, and the (O) letter means that the specimen has an opening, while (2, 4, R, 4R) represent slabs strengthened with two, four, rhombus-shape, or four with rhombus-shape metal straps around the openings respectively. The symbols (MM, MC, and CC) indicate the location of the openings either in the Middle strip -Middle strip, Middle strip -Column strip, or Column strip -Column strip respectively.

2.2 Details of slab reinforcement and strain gauges

The primary reinforcing steel bars utilized in this study were deformed bars with a diameter of 10 mm. which are interconnected with steel wires to form a mesh of reinforcement having 160 mm center to center in both directions at the bottom face having hooks at the ends as an anchorage as shown in Figure 1. The specification of the steel bars is shown in Table 2. The steel bar strain gages used in the slabs are of type BF-120-3AA-TO-G-P5K having 10 mm length, gage factor 2.11 ±1 % (sensitivity of the strain gages) and gage resistance 120 Ω ± 0.5 Ω. The steel strain gages were affixed on the tension side of the bars after the bars smoothened and cleaned well at the deformed ribs to connect firmly with the strain gages. A special water-resistant glue was used for this connection process to prevent any absorption of moisture.

2.3 Concrete mixture

The ingredients required for this mix are tabulated in Table 3. Ordinary Portland Cement was used, the coarse aggregate having maximum aggregate size 12.5 mm with water absorption 0.6% and fine aggregate having fineness modulus 2.61 with water absorption 1.66% were utilized. The cylindrical compressive strength of the mixture was (31.8 MPa) after 28 days of curing, the sieve analysis complies with ASTM C33[19].

2.4 Heavy-Duty Metal Strap (HDMS)

In this research, HDMS were used for strengthening the specimens that have openings in different locations to restore capacity of the slabs as shown in Figure 2. Specifications of the metal straps are illustrated in Table 4. The stress-strain diagram also shown in Figure 3, to show the capability of the material. The metal straps are black-painted and waxed, and the dimensions are 32 mm wide and 0.8 mm thick. This strengthening technique are used by mechanical bond between the metal straps and the concrete through thru bolts which are having 10 mm diameter and 80 mm length as shown in Figure 4. The process first made by cleaning the surface of the concrete and smoothening the face, making holes on the tension side of concrete with depth 45 mm using drill machine, putting the anchor bolts in their pre-indicated positions in the holes, then hammering them into the slab, putting the metal straps on the outer side of the anchor bolts then fastening them using fastener machine and affixing each on the surface of the slabs tightly.

2.5 Test Setup

As shown in Figure 5, a steel frame was used to perform the experiment but some modifications were made to the frame to fit the test as a steel frame was built for the slabs with IPE240 steel section and a 32mm diameter solid rode under the specimens. A hydraulic loading jack with 1000 kN capacity was used and a box steel was attached to this jack then a load cell with capacity of 300 kN was utilized but a steel plate having dimensions (350×350×25) mm was attached to the load cell to be put on the surface of the slabs for the purpose of transferring the load onto the specimens, considering the positions of the openings

in the slabs. The data were obtained using a data logger that was connected to a computer also an LVDT was attached to the surface of the slabs on an independent frame to compute the deflection of the slabs at each reading parallel to the load data, concrete strain gages were affixed on the bottom surface of the specimens to show the strain values in the concrete, and steel strain gages were attached to the tension side of the metal straps for demonstrating the strain in them during all the phases of the loadings.

3. Results and Discussions

The results of the test are compared to demonstrate the efficacy of the strengthening technique. The test aimed to know the effect of the strengthening on the enhancement of the load-carrying capacity and controlling the deflection in each specimen. Table 5 shows the results of the test.

3.1 Load-Deflection, Stiffness, and Ductility

The load–deflection curves as shown in Figure 6, is used to compare the global flexural response of the tested two-way slabs from first cracking to the ultimate state. For each specimen, the cracking load P_{cr} marked the onset of visible cracking, while a yield point was defined by $P_y = 0.75P_u$ to enable consistent comparisons when a distinct yield point was not obvious on the curves [4] . The associated yield deflection Δ_y and ultimate deflection Δ_u were taken from the recorded data. The yield stiffness $K_y = P_y/\Delta_y$ represents the stiffness level up to the effective yield point, whereas the ultimate stiffness $K_u = (P_u - P_y)/(\Delta_u - \Delta_y)$ captured the slope between the effective yield and the peak response. The ductility index $DI = \Delta_u/\Delta_y$ quantifies the deformation capacity beyond the yield stage, and the residual stiffness value provided an additional indicator of the stiffness retained toward the later stages of response.

3.1.1 Control solid slab SCSU

The control solid slab (SCSU) provided the benchmark load–deflection behaviour for all specimen comparisons. It developed $P_{cr} = 34.60$ kN, then reached $P_y = 135.71$ kN at $\Delta_y = 6.85$ mm, indicating a relatively stiff response prior to the effective yield point $(K_y = 19.81\ kN/mm)$. The slab then attained the maximum load $P_u = 180.95$ kN at $\Delta_u = 10.41$ mm. The calculated $DI = 1.52$ showed that the deformation capacity beyond the yield stage was limited. The post-yield stiffness $(K_u = 12.71\ kN/mm)$ and residual stiffness (7.10)indicated that the slab retained a comparatively high slope into the advanced loading stages, consistent with the reference response observed in the load–deflection curve.

3.1.2 Group I (Middle strip - Middle strip)

SCOUMM: -

Introducing the Middle strip -Middle strip group opening without strengthening reduced the load capacity and increased the deformation demand relative to the control solid slab. SCOUMM reached $P_{cr} = 21.88$ kN, which was lower than SCSU, indicating earlier crack initiation around the weakened region. The effective yield point occurred at $P_y = 107.81$ kN and a relatively large $\Delta_y = 8.75$ mm, giving a lower yield stiffness $(K_y = 12.32\ kN/mm)$ than the control solid slab. The peak response was $P_u = 143.74$ kN (79% of SCSU) at a markedly larger $\Delta_u = 15.78$ mm, showing that the specimen sustained load at a higher deflection demand. Although the ultimate load decreased, the deformation capacity increased $(DI = 1.80)$, while the ultimate stiffness reduced significantly $(K_u = 5.11\ kN/mm)$, consistent with the flatter slope of the curve after extensive cracking. The residual stiffness value of 7.21 indicated that the specimen still retained a measurable stiffness contribution at late stages, but the overall response remained less stiff than the control solid slab.

SSO2MM: -

SSO2MM showed a different behaviour compared with SCOUMM, with a higher cracking resistance and an earlier engagement of stiffness in the pre-yield response. It developed $P_{cr} = 45.72$ kN, exceeding both SCOUMM and the control solid slab, which indicated delayed crack initiation under the adopted HDMS arrangement. The specimen reached $P_y = 105.32$ kN at $\Delta_y = 6.00$ mm, producing a higher yield stiffness $(K_y = 17.55\ kN/mm)$ than SCOUMM and a yield deflection closer to the control solid slab. The peak load was $P_u = 140.42$ kN (78% of SCSU and 97.69% of SCOUMM) at $\Delta_u = 10.84$ mm, meaning that the specimen reached its maximum load at a substantially lower deflection than the unstrengthened reference. This balance produced $DI = 1.81$with a relatively stable post-yield slope $(K_u = 7.25\ kN/mm)$ and a higher residual stiffness (10.30)than SCOUMM.

SSO4MM: -

SSO4MM exhibited early cracking and a high deformation demand to reach both the effective yield and the ultimate state. The cracking load dropped to $P_{cr} = 12.96$ kN, which was lower than both SCOUMM and SCSU, indicating that crack initiation occurred at a relatively low load level. The slab reached $P_y = 110.34$ kN at a large $\Delta_y = 11.00$ mm, resulting in a lower yield stiffness $(K_y = 10.03\ kN/mm)$and a yield deflection noticeably higher than the control solid slab. The ultimate response increased slightly relative to SCOUMM, reaching $P_u = 147.12$ kN (81% of SCSU and 102.35% of SCOUMM), but this occurred at $\Delta_u = 17.67$ mm. Consequently, the deformation capacity beyond the yield point was moderate

($DI = 1.61$), while the post-yield stiffness remained low ($K_u = 5.51\ kN/mm$), consistent with a curve that extended further in deflection as cracking accumulated. The residual stiffness value was 4.52, suggesting limited stiffness retention toward the final stages.

SSORMM: -

SSORMM followed a similar trajectory to SSO4MM, with early crack initiation and large deformation demand before peak load. It developed $P_{cr} = 20.00$ kN, which remained below the control solid slab and below SSO2MM and SSO4RMM. The yield point was $P_y = 108.90$ kN at $\Delta_y = 10.68$ mm, giving $K_y = 10.20\ kN/mm$, again reflecting a softer pre-yield response than SCSU. The specimen attained $P_u = 145.20$ kN (80% of SCSU and 101.02% of SCOUMM) at $\Delta_u = 16.86$ mm, confirming that the slight gain in peak load within the group was achieved with a substantial increase in deflection demand. The ductility index was $DI = 1.58$, and the post-yield stiffness was $K_u = 5.87 kN/mm$, which together described a response that relied more on deformation spread than on strength recovery. The residual stiffness (4.32) was also low, consistent with reduced stiffness retention near the end of the curve.

SSO4RMM: -

SSO4RMM showed the clearest restoration of load capacity within Group I while maintaining a relatively controlled deflection demand compared with the highly deformable MM specimens. It achieved $P_{cr} = 47.30$ kN, indicating delayed crack initiation similar to SSO2MM and higher than both SCOUMM and SCSU. The effective yield point occurred at $P_y = 120.23$ kN with $\Delta_y = 5.95$ mm, giving the highest yield stiffness in the group ($K_y = 20.21\ kN/mm$) and a yield deflection close to the control solid slab. The peak response reached $P_u = 160.30$ kN (89% of SCSU and 111.52% of SCOUMM) at $\Delta_u = 11.36$ mm, indicating that the added load capacity within Group I was not accompanied by the large deflection observed in SSO4MM and SSORMM. This combination produced $DI = 1.91$ and a stable ultimate stiffness ($K_u = 7.41\ kN/mm$), together with a high residual stiffness value (12.80), suggesting sustained stiffness contribution at advanced load levels. From an installation standpoint, this response was consistent with an interpretation that the HDMS system in SSO4RMM may have engaged earlier and more uniformly attached to the bottom surface of the slab, where tighter and more consistent clamping could have reduced seating slip and increased the effective participation of the straps in restraining crack opening and deflection growth.

3.1.3 Group II (Column strip - Column strip)

SCOUCC: -

Relative to the control solid slab, SCOUCC retained a high peak load but exhibited an increased deformation demand. It developed $P_{cr} = 12.20$ kN, indicating early cracking. The effective yield point was $P_y = 130.50$ kN at $\Delta_y = 8.60$ mm, giving $K_y = 15.17\ kN/mm$, which was lower than the control solid slab due to the larger yield deflection. The specimen reached $P_u = 174.00$ kN (96% of SCSU) at $\Delta_u = 14.26$ mm, showing that the peak capacity remained close to the control solid slab, while the deflection demand increased by about 37% relative to SCSU. The ductility index was $DI = 1.66$, and the post-yield stiffness was $K_u = 7.69\ kN/mm$, consistent with the load-deflection graph that extended further in deflection while sustaining high loads. The residual stiffness (7.49) indicated moderate stiffness retention toward the late stages.

SSO4CC: -

SSO4CC showed its primary strengthening influence early in the response, where the curve shifted upward in the cracking region and reached the yield point at a lower deflection than the unstrengthened baseline. The cracking load increased to $P_{cr} = 35.60$ kN, which was close to the control solid slab and far higher than SCOUCC, indicating delayed crack initiation. The effective yield point occurred at $P_y = 126.08$ kN with $\Delta_y = 6.70$ mm, resulting in a higher yield stiffness ($K_y = 18.82\ kN/mm$) and a yield deflection that was lower than SCOUCC, meaning the specimen required less deformation to reach the yield stage and remained stiffer through that portion of the curve. The ultimate load was $P_u = 168.10$ kN (93% of SCSU and 96.61% of SCOUCC) at ultimate deflection $\Delta_u = 13.60$ mm, indicating that the strengthened response emphasised improved crack control and a stiffer trajectory in the first half of the load–deflection history, while the peak load within the group remained slightly below the unstrengthened baseline. The deformation capacity remained high ($DI = 2.03$), and the post-yield stiffness ($K_u = 6.09\ kN/mm$) together with the high residual stiffness (12.73) supported the observation that stiffness retention toward later stages was enhanced relative to SCOUCC, even though peak load did not increase.

SSO2CC: -

SSO2CC showed a different strengthening outcome, where the peak load was sustained at a slightly higher level than the unstrengthened baseline but with a pronounced development in deflection capacity. The cracking load was $P_{cr} = 17.00$ kN, which remained low compared with SSO4CC, indicating that this configuration did not delay crack initiation to the same extent. The yield point occurred at $P_y = 131.85$ kN and $\Delta_y = 8.50$ mm, producing $K_y = 15.51\ kN/mm$, which was close to SCOUCC and reflected a

similar deformation requirement to reach the yield stage. The specimen attained $P_u = 175.80$ kN (97% of SCSU and 101.03% of SCOUCC) at $\Delta_u = 17.30$ mm, meaning that it sustained a slightly higher peak load than the unstrengthened baseline while extending the curve substantially in deflection. This led to $DI = 2.04$ and a lower post-yield stiffness ($K_u = 4.99 kN/mm$), indicating that the additional deformation capacity was achieved with a flatter slope of the curve after the yield point. The residual stiffness (10.52) remained higher than SCOUCC, consistent with a strengthening contribution that supported continued load carrying at larger deflections. Overall, within Group II, the load–deflection results showed that the HDMS strengthening was reasonably effective, with SSO4CC expressing the effect most clearly in the early cracking and yield portion of the curve, whereas SSO2CC expressed the effect mainly through sustaining peak load while extending the deformation range.

3.1.4 Group III (Middle strip - Column strip)

SCOUMC: -

SCOUMC provided the baseline behaviour for specimens with openings located closer to the slab support zones (middle strip–column strip). It developed a relatively high cracking load $P_{cr} = 45.30$ kN, then reached $P_y = 111.30$ kN at $\Delta_y = 4.70$ mm, giving a high yield stiffness ($K_y = 23.68 kN/mm$), which indicated a stiff response up to the effective yield point. The ultimate load was $P_u = 148.40$ kN (82% of the control solid slab) at $\Delta_u = 9.86$ mm, showing that the specimen sustained its peak load at a moderate deflection. The ductility index was $DI = 2.10$, reflecting that the specimen still developed a considerable deformation capacity beyond the yield stage despite its relatively stiff early response. The ultimate stiffness ($K_u = 7.19 kN/mm$) and the high residual stiffness (16.49) indicated that the specimen retained notable stiffness toward the later stages, which aligned with the distributed cracking observed on the bottom face after testing.

SSO2MC: -

SSO2MC, strengthened using two straps anchored by four through-bolts, exhibited a reduction in both peak load and deformation capacity relative to the unstrengthened baseline. The cracking load decreased to $P_{cr} = 39.80$ kN, indicating earlier crack initiation than SCOUMC. The effective yield point occurred at $P_y = 105.35$ kN and $\Delta_y = 4.40$ mm, which kept the yield deflection close to the baseline specimen (SCOUMC) but slightly reduced the yield stiffness only marginally upward ($K_y = 23.94 kN/mm$) due to the smaller Δ_y. The ultimate load reached $P_u = 140.46$ kN, corresponding to 78% of the control solid slab and 94.65% of SCOUMC, at a reduced $\Delta_u = 7.20$ mm, indicating that the specimen peaked at a smaller deformation demand than the baseline. The lower $DI = 1.64$ described a reduced deformation reserve beyond yield compared with SCOUMC. The post-yield stiffness increased ($K_u = 12.54 kN/mm$), which was consistent with a steeper slope between yield and peak load over a shorter deflection interval, while the residual stiffness reduced to 11.40, indicating less stiffness retention at the late stages than the unstrengthened specimen.

SSO4MC: -

SSO4MC used a more developed HDMS layout around the opening and was anchored using 8 through-bolts, which influenced both cracking distribution and deformation development. The cracking load was $P_{cr} = 33.30$ kN, lower than both SCOUMC and SSO2MC, indicating that crack initiation occurred earlier in this configuration. The specimen reached $P_y = 105.59$ kN at a larger $\Delta_y = 5.20$ mm, giving a reduced yield stiffness ($K_y = 20.30 kN/mm$)compared with SCOUMC and SSO2MC. The ultimate load was $P_u = 140.78$ kN (78% of the control solid slab and 94.87% of SCOUMC), essentially similar to SSO2MC in peak load, but it occurred at a much larger $\Delta_u = 12.82$ mm. This shift increased the ductility index to $DI = 2.47$, indicating a substantial deformation reserve beyond the yield stage. The post-yield stiffness decreased to $K_u = 4.62 kN/mm$, consistent with a flatter slope after yield as cracking propagated and the response extended further in deflection. The residual stiffness remained high (15.69), indicating that despite the lower initial cracking resistance, the specimen retained stiffness contribution in the later stages.

3.2 Crack Pattern and Mode of Failure

Figure 7, shows the crack pattern of each specimen after the test. The patterns show the initiation of the cracks from the start to the final depiction, then indication of the failure modes is discussed on that basis. For clarity, Flexural failure mode is a bending-controlled collapse in which tensile cracks form and progressively widen in the tension zone, then a few dominant cracks connect to create a yield-line type pattern across the slab. This mode is usually accompanied by relatively large deflections, gradual stiffness reduction, and visible warning through crack development and deformation. Punching shear failure mode is a localized shear-controlled failure concentrated around the loaded area (or a column/bearing plate), where a critical diagonal crack forms through the slab thickness and a cone- or pyramid-shaped region tends to separate. It typically occurs with limited warning, smaller additional deflection near failure, damage concentrated near the load, and a sudden drop in load capacity.

3.2.1 SCSU

The control solid slab developed a classical two-way flexural crack field on the tension face, with cracks

initiating after the first cracking load and then extending along the principal bending directions as the load increased. With further loading, cracking intensified in the central region and stiffness degraded progressively until the ultimate load was reached at a moderate maximum deflection. The observed damage at the end of the test was consistent with a flexure-dominated response with localized severe distress at the loaded zone, which could be described conservatively as a flexure–punching interaction rather than a purely flexural failure.

3.2.2 GROUP I (Middle strip - Middle strip)

SCOUMM: -

Introducing the middle strip–middle strip opening shifted crack initiation to the re-entrant corners of the opening and reduced the cracking load compared with the control solid slab. The crack pattern typically concentrated around the opening corners and then propagated into the slab panel, indicating that the opening interrupted the stress flow and forced higher tensile demand into the remaining concrete ligaments. The relatively large ultimate deflection suggested a deformation-controlled response, and the mode of failure was interpreted as flexural cracking governed by the weakened ligament around the opening, followed by crushing/localized damage near the critical zone at peak load.

SSO2MM: -

This specimen showed delayed crack initiation relative to the unstrengthened SCOUMM specimen, indicating that the two-strap HDMS system contributed to restraining tensile opening and delaying the formation of major cracks at the opening corners. After cracking, the curve maintained a stable load increase up to the effective yield and ultimate states with a maximum deflection close to the control solid slab, implying that cracking remained comparatively controlled and did not require excessive deformation to mobilize resistance. The failure mode was assessed as flexure-dominated, governed by cracking at the opening corners and the adjacent ligament, without evidence from the response of a brittle punching-type collapse.

SSO4MM: -

Although HDMS was present, this specimen exhibited an early crack initiation and then developed a response characterized by a high deformation demand to reach yield and ultimate conditions. Such behaviour was consistent with wide crack opening and progressive redistribution through multiple cracks, which can occur when strap engagement was delayed by seating or partial slip at the strap–concrete interface. The final condition corresponded to a flexural failure mode controlled by the opening region, but with larger crack widths and a more pronounced softening trend that reflected reduced crack-control efficiency compared with the tighter configurations.

SSORMM: -

SSORMM followed a similar cracking scenario to SSO4MM, with relatively low cracking load and a large deformation demand at yield and ultimate. The pattern implied that cracks initiated early at the opening corners and then spread through the panel as load increased, with the strengthening contribution becoming fully effective only after noticeable deformation accumulated. The mode of failure was therefore interpreted as flexural cracking governed by the opening-weakened ligament, accompanied by large crack development prior to peak load.

SSO4RMM: -

This configuration delayed cracking to a level comparable with the strongest MM responses and achieved a higher retained ultimate capacity than the other strengthened MM specimens while keeping the maximum deflection relatively close to the control solid slab. The combined response indicated improved crack control and earlier strap engagement. In practical terms, this was consistent with a more uniform and tighter HDMS fixing, which would reduce interface slip and limit crack localization. The failure mode remained flexure-dominated around the opening, but with a more controlled crack pattern and less extreme deformation at peak load than SSO4MM and SSORMM.

3.2.3 GROUP II (Column strip - Column strip)

SCOUCC: -

For SCOUCC, the bottom-face cracking developed as a distributed two-way flexural crack field that was strongly governed by the presence of the opening. Cracks initiated primarily at the re-entrant corners of the opening and along the adjacent concrete ligaments, then propagated outward into the slab panel with branching and intersection of secondary cracks. With increasing load, several dominant cracks extended toward the slab edges while additional diagonal cracks formed, indicating progressive stiffness degradation and redistribution of internal forces rather than sudden localized collapse. The widespread cracking over a large portion of the slab, together with the absence of a clearly concentrated failure zone, supported a flexure-dominated mode of failure controlled by the opening-corner and ligament action, potentially accompanied by minor local shear effects, but not a pure punching-type failure.

SSO2CC: -

The observed cracking on the tension face formed a two-way flexural crack field that spread from the highly stressed central region toward the slab edges, while the opening introduced local stress concentration at its re-entrant corners. The crack map showed multiple intersecting and branching cracks, with several dominant cracks extending across the panel and secondary cracks developing around the

opening perimeter. Compared with the unstrengthened SCOUCC specimen, the presence of the HDMS strips and through-bolts promoted earlier crack between several paths near the opening zone, so the cracking became more distributed and less dominated by one ligament; however, a few major cracks still governed the late-stage response by linking the central region to the slab boundaries. Based on the wide spread of flexural cracks across the slab and the absence of a clearly isolated local cone at the loaded region, the failure was interpreted as flexure-dominated two-way action influenced by the opening, with possible local shear participation near the opening corners, rather than a purely punching-type failure.

SSO4CC: -

In SSO4CC, the cracking pattern remained predominantly flexural, but the early-stage cracking near the critical region appeared better regulated: instead of immediately localizing into one dominant path, the cracks spread into a wider fan and multiple branches formed across the slab. Around the opening, diagonal cracks still originated from the re-entrant corner, but several cracks deviated, terminated, or changed direction near the HDMS lines and the thru-bolt anchorage points, indicating that the strengthening system engaged and influenced the crack trajectories. In the later stages, one main crack line became dominant and widened, while secondary cracks continued to develop away from it, reflecting redistribution of tensile demand before final failure.

3.2.4 Group III (Middle strip - Column strip)

SCOUMC: -

Because the opening was closer to the support region, cracking concentrated strongly in the reduced ligament between the opening and the main span. The crack map shows two dominant “strip-type” cracks developing below the opening, accompanied by fan-shaped cracks spreading toward the edges. This is typical of a slab that is forced to transfer load through a narrower effective strip, which raises curvature demand and promotes earlier localisation. The end condition is best described as flexure-controlled in the remaining strip, with local flexure–shear interaction at the opening corners (stress concentration at the re-entrant corners), rather than a pure punching failure.

SSO2MC: -

In specimen SSO2MC, cracking initiated primarily at the re-entrant corners of the square opening due to stress concentration, then propagated outward as a combination of inclined diagonal cracks from the opening corners and flexural cracks aligned with the principal bending directions. With further loading, several cracks became dominant and formed a clear yield-line type pattern, indicating progressive stiffness degradation and segmental rotation of the slab panels. The observed crack distribution and the development of long, through cracks extending toward the boundaries suggest a predominantly flexure-controlled (two-way) failure mechanism, while the opening mainly influenced the location and severity of cracking rather than producing a distinct localized punching cone.

SSO4MC: -

SSO4MC exhibited a denser crack pattern and more branching near the strengthened region and the ligament below the opening, while reaching an ultimate load similar to SSO2MC. The higher crack density could be interpreted as improved redistribution and crack dispersion due to the additional strap lines; however, the presence of 8 thru-bolts also introduced more penetrations in a highly stressed ligament, which could have promoted multiple crack initiations and local weakening around bolt holes. The combined evidence therefore supported a flexure-dominated failure mechanism in which the strap layout promoted wider crack distribution, while the bolt-anchorage discontinuities and the opening position limited the achievable gain in ultimate capacity.

4. Conclusion

- The experimental results confirm that introducing openings reduced the ultimate capacity and stiffness of the tested two-way slabs compared with the solid control specimen, and that the effectiveness of HDMS depended strongly on the opening location and the selected strap configuration.
- For the Middle strip–Middle strip opening group, strengthening did not always produce a clear increase in ultimate capacity; however, the optimized arrangement SSO4RMM achieved the best recovery among the specimens of Group I, reaching about 89% of the control capacity and providing the strongest stiffness restoration as compared with the specimens of the same group.
- For the Column strip–Column strip opening group, the behaviour was the most consistent, with ultimate capacities remaining high at about 93–97% of the control, together with noticeable improvement in cracking resistance and ductility.
- For the Middle strip–Column strip opening group, the ultimate capacity remained around 78% of the control, while the response was configuration-dependent: one layout showed near restoration of ultimate stiffness, whereas another achieved the highest ductility among all specimens.
- Overall, HDMS is a practical strengthening technique for slabs with openings, but its benefits depend on the configuration and application method; the strengthening layout must be selected, tightening the straps must be checked and fixed firmly to match the governing load-transfer path for each opening position.

Recommendations

- For practical strengthening, selection and detailing the HDMS layout according to the opening location (e.g., Column strip–Column strip versus Middle strip–Column strip) must be studied, ensuring symmetry where applicable, reliable anchorage, and alignment with the main bending directions to obtain stable stiffness and ductility recovery.
- Future research should quantify the influence of detailing parameters (strap spacing, bolt arrangement, and strap distance from opening corners) on strength recovery and on the transition between flexure-dominated and punching-shear-dominated behaviour, supported by strain monitoring and validated numerical modeling.

References

[1] S.-C. Floruț, T. Nagy-György, V. Stoian, and D. Dan, "On The Issue of RC Slabs with Cut-Out Openings Retrofitted by Means of CFRP Systems," in *12th International Conference on Steel, Space and Composite Structures*, Prague, May 2014, pp. 1–6. [Online]. Available: http://www.upt.ro

[2] ACI Committee 318, "Building Code Requirements for Structural Concrete (ACI 318M-25) and Commentary (ACI 318RM-25)," Farmington Hills, MI, USA, 2025.

[3] "Eurocode 2: Design of concrete structures-Part 1-1: General rules and rules for buildings," 2010.

[4] E. H. El-Mawsly, K. F. O. El-Kashif, A. A. Shawky, and H. A. Abdalla, "Experimental and numerical investigation on strengthening of RC flat slabs with central opening," *Case Studies in Construction Materials*, vol. 16, Jun. 2022, doi: 10.1016/j.cscm.2022.e00974.

[5] H. Chand Dewangan, S. Kumar Panda, and C. Kumar Hirwani, "Numerical deflection and stress prediction of cutout borne damaged composite flat/curved panel structure," *Structures*, vol. 31, pp. 660–670, Jun. 2021, doi: 10.1016/j.istruc.2021.02.016.

[6] D. K. Nageswara Rao, M. Ramesh Babu, K. Raja Narender Reddy, and D. Sunil, "Stress around square and rectangular cutouts in symmetric laminates," *Compos Struct*, vol. 92, no. 12, pp. 2845–2859, Nov. 2010, doi: 10.1016/j.compstruct.2010.04.010.

[7] R. H. Abu-Zeyad, A. A. El-Ashal, N. H. Abdel-Mutaal, and N. H. Amer, "Experimental Analysis of Centrally Openned Two-Way Slabs Strengthened with Carbon Fiber Laminates," in *6th International Conference on Civil & Architecture Engineering (ICCAE)*, Cairo, May 2006, pp. 209–221.

[8] N. K. and S. T. S. Oukaili, "Punching shear strength of reinforced concrete flat plates with opening," *Journal of Engineering*, vol. 20, pp. 1–20, 2014.

[9] O. Enochsson, "CFRP Strengthening of Concrete Slabs, with and without Openings Experiment, Analysis, Design and Field Application (Licentiate thesis, no. 2005:87)," Thesis, Luleå University of Technology, Luleå, 2005. [Online]. Available: www.cee.ltu.se

[10] S. S. Aman, B. S. Mohammed, M. A. Wahab, and A. Anwar, "Performance of reinforced concrete slab with opening strengthened using CFRP," *Fibers*, vol. 8, no. 4, Apr. 2020, doi: 10.3390/fib8040025.

[11] H. Saadatmanesh and A. M. Malek, "Design Guidelines for Flexural Strengthening of RC Beams with FRP Plates," *Journal of Composites for Construction*, vol. 2, no. 4, pp. 158–164, 1998, doi: 10.1061/(ASCE)1090-0268(1998)2:4(158).

[12] M. R. Mostakhdemin Hosseini, S. J. E. Dias, and J. A. O. Barros, "Flexural strengthening of pre-cracked RC slabs with prestressed NSM CFRP laminates and evaluation of strain loss," *Advances in Structural Engineering*, vol. 24, no. 13, pp. 2927–2947, Oct. 2021, doi: 10.1177/13694332211010585.

[13] H. Pham and R. Al-Mahaidi, "Assessment of available prediction models for the strength of FRP retrofitted RC beams," *Compos Struct*, vol. 66, no. 1–4, pp. 601–610, Oct. 2004, doi: 10.1016/j.compstruct.2004.05.008.

[14] M. Mahlis, A. E. Shoeib, S. Abd Elnaby, and A. Sherif, "The Effect of Cutting Openings on the Behavior of Two-way Solid Loaded Slabs," *Structures*, vol. 16, pp. 137–149, Nov. 2018, doi: 10.1016/j.istruc.2018.09.002.

[15] D. Banu, N. Ţăranu, and R. Carneiro, "Experimental Study on Two Way Reinforced Concrete Slabs with or without Openings Strengthened with Composite Strips. A: Experimental Setup," *Buletinul Institutului Politehnic din Iași*, vol. 58, no. 2, pp. 88–96, 2012, [Online]. Available: https://www.researchgate.net/publication/261456089

[16] Walid. Elsayed, *Strengthening of reinforced concrete two-way slabs using mechanically fastened FRP systems = Renforcement de dalles armées bidirectionnelles avec des systèmes de PRF attachés mécaniquement*. Library and Archives Canada = Bibliothèque et Archives Canada, 2008.

[17] R. P. Neupane, T. Imjai, and R. Garcia, "A novel post-tensioned metal strapping

البلاطات الخرسانية المسلحة ثنائية الاتجاه ذات الفتحات والمقوّاة باستخدام أشرطة معدنية عالية التحمل

المستخلص

تُنفَّذ الفتحات في البلاطات الخرسانية المسلحة عادةً لتسهيل مرور الخدمات الميكانيكية والكهربائية؛ غير أنها تؤدي إلى انخفاض ملحوظ في الصلابة، وقدرة التحمل، واللدونة، مما قد يغيّر من آلية الفشل المسيطرة. في هذه الدراسة، تم إجراء تحليل تجريبي لاثنتي عشرة بلاطة خرسانية مسلحة ثنائية الاتجاه، شملت بلاطة صلبة مرجعية، وثلاث بلاطات غير مُقوّاة تحتوي على فتحات في مواقع مختلفة (وسط،ركن،وحافة)، وثماني بلاطات مُقوّاة باستخدام أشرطة معدنية عالية التحمل (HDMS) و هي شرائط رقيقة من الفولاذ تثبت خارجيا وتستخدم كنظام تقوية، أظهرت النتائج أن البلاطات غير المُقوّاة ذات الفتحات سجّلت انخفاضاً كبيراً في الحمل الأقصى بلغ حتى ٢٠٪ مقارنة بالبلاطة الصلبة المرجعية، إضافةً إلى انخفاض الصلابة الانحنائية، مع تحوّل أنماط الفشل بشكل رئيسي نحو القص الثاقب. استُعيدت مقاومة البلاطات ذات الفتحات الركنية إلى مستوى قريب من البلاطة المرجعية، مع زيادة في الصلابة تجاوزت ٤٠٪ وتحسن في الأداء اللدن. أما في حالة الفتحات الوسطية، فقد تحقق استرجاع جزئي لكل من الصلابة والحمل الأقصى، مصحوباً بزيادة كبيرة في اللدونة. وفيما يتعلق بالفتحات الجانبية، فقد اعتمدت فعالية الأشرطة المعدنية بدرجة كبيرة على نمط التوزيع؛ حيث تمكّن الترتيب الأمثل من استعادة الصلابة القصوى إلى مستوى مقارب للبلاطة المرجعية، في حين أظهرت الترتيبات الأخرى فوائد محدودة.

الكلمات المفتاحية:

البلاطات ثنائية الاتجاه , الفتحات التقوية , الأداء الإنشائي , الأشرطة المعدنية عالية التحمل

technique to actively confine concrete structures: a review," *Innovative Infrastructure Solutions*, vol. 10:16, 2025, doi: 10.1007/s41062-024-01791-0.

[18] T. Imjai, U. Chaisakulkiet, R. Garcia, and K. Pilakoutas, "Strengthening of RC members using post-tensioned metal straps: state of the research," *International Association of Lowland Technology*, vol. 20, no. 2, pp. 187–196, Sep. 2018.

[19] ASTM International, "Standard Specification for Concrete Aggregates (ASTM C33/C33M-13)," ASTM International, West Conshohocken, PA, Jan. 2013. doi: 10.1520/C0033_C0033M-13.

Table 1. Detail of the specimens

Group	Specimen abbreviation	Opening size (mm)	Strengthening Technique	Strengthening configuration
-	SCSU	No	No	Slab Control Solid unstrengthened
I	SCOUMM	250 × 250	No	Slab Control with opening at middle strip-middle strip unstrengthened
	SSO2MM	250 × 250	HDMS	Slab strengthened with 2 heavy-duty metal straps having opening at middle strip-middle strip
	SSO4MM	250 × 250	HDMS	Slab strengthened with 4 heavy-duty metal straps having opening at middle strip-middle strip
	SSORMM	250 × 250	HDMS	Slab strengthened with 4 rhombus-shape heavy-duty metal straps having opening at middle strip-middle strip
	SSO4RMM	250 × 250	HDMS	Slab strengthened with a mix of 4 straight and 4 rhombus-shape heavy-duty metal straps having opening at middle strip-middle strip
II	SCOUCC	250 × 250	No	Slab Control with opening at column strip-column strip unstrengthened
	SSO2CC	250 × 250	HDMS	Slab strengthened with 2 heavy-duty metal straps having opening at column strip-column strip
	SSO4CC	250 × 250	HDMS	Slab strengthened with 4 heavy-duty metal straps having opening at column strip-column strip
III	SCOUMC	250 × 250	No	Slab Control with opening at middle strip-column strip unstrengthened
	SSO2MC	250 × 250	HDMS	Slab strengthened with 2 heavy-duty metal straps having opening at middle strip-column strip
	SSO4MC	250 × 250	HDMS	Slab strengthened with 4 heavy-duty metal straps having opening at middle strip-column strip

Table 2. Characteristics of the reinforcing bars

Diameter (mm)	Cross-section Area (mm2)	Yield Strength (MPa)	Ultimate Strength (MPa)	Elongation (%)
10	78.5	540	639	13

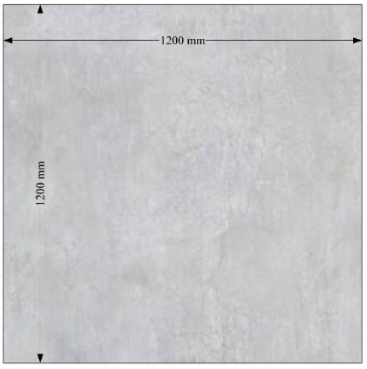

a1. Bottom view of SCSU

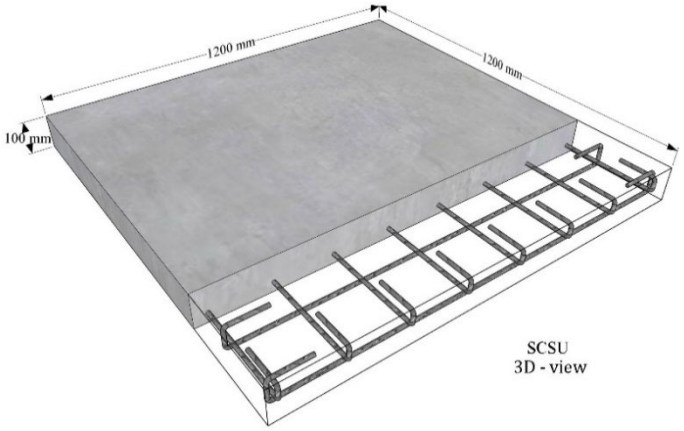

a2. 3D view of SCSU

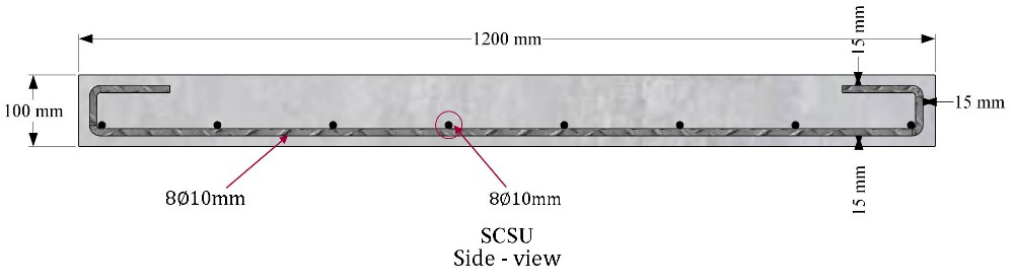

a3. Section of SCSU

a. Detail of the SCSU specimen

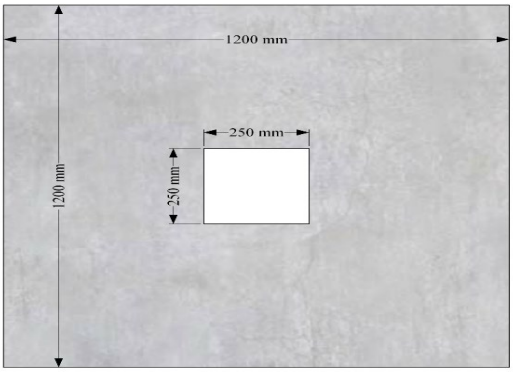

SCOUMM
Bottom-View

b1. Bottom view of SCOUMM

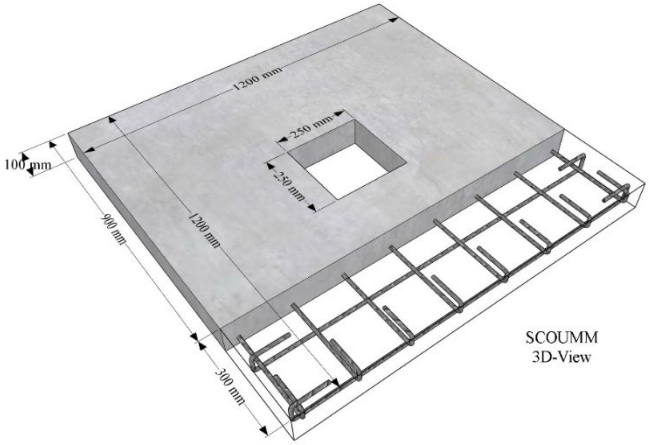

b2. 3D view of SCOUMM

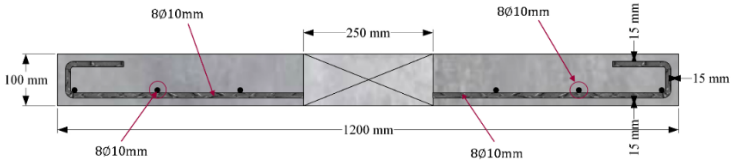

SCOUMM
Side-View

b3. Section of SCOUMM

b. Detail of the SCOUMM specimen

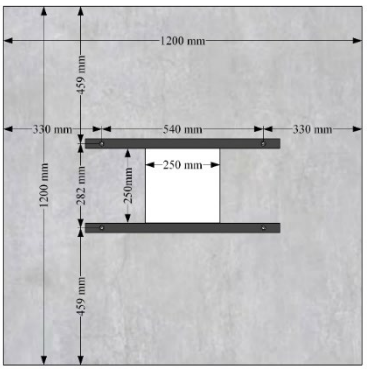

SSO2MM
Bottom-View

c1. Bottom view of SSO2MM

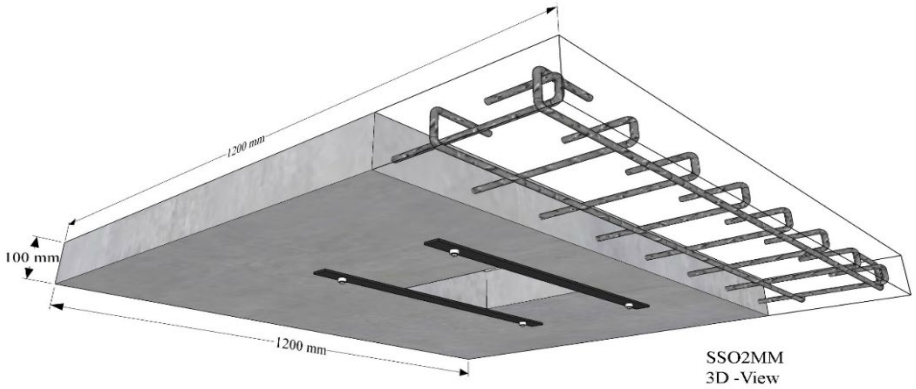

SSO2MM
3D -View

c2. 3D view of SSO2MM

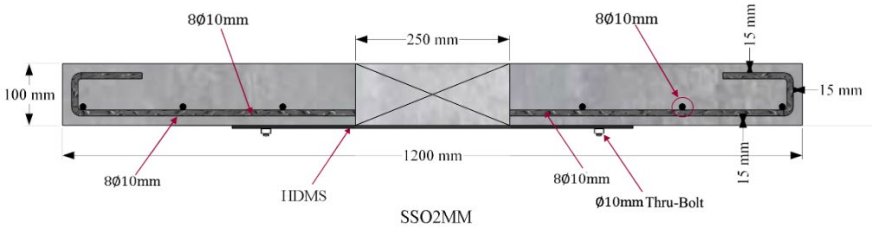

SSO2MM
Side-View

c3. Section of SSO2MM

c. Detail of the SSO2MM specimen

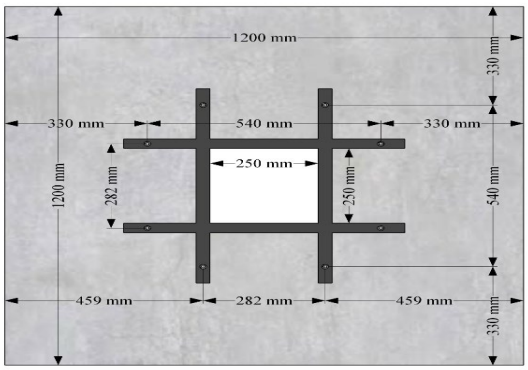

SSO4MM
Bottom-View

d1. Bottom view of SSO4MM

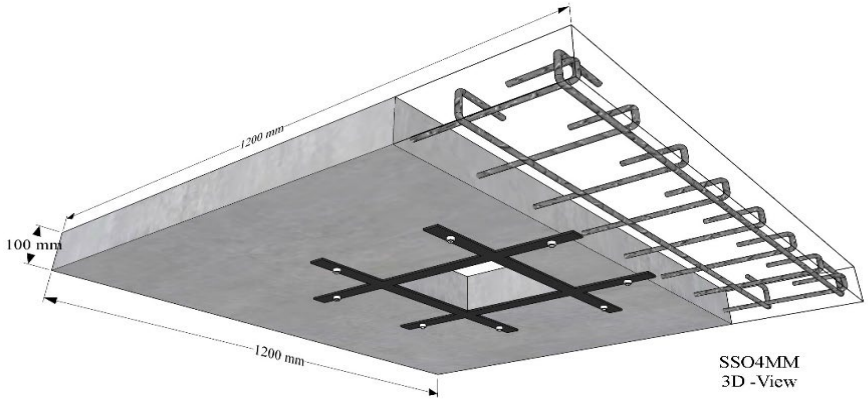

d2. 3D view of SSO4MM

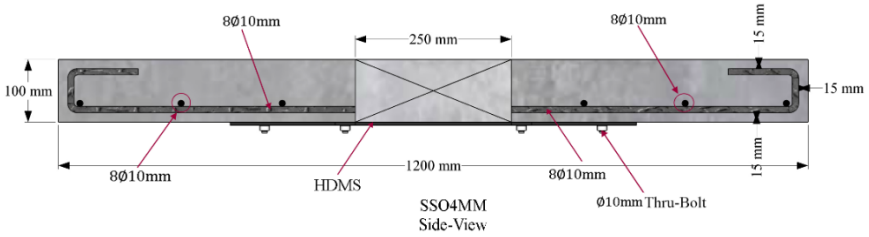

d3. Section of SSO4MM

d. Detail of the SSO4MM specimen

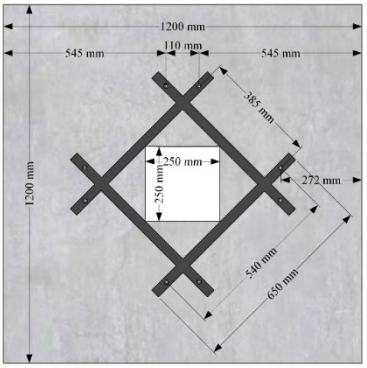

SSORMM
Bottom -View

e1. Bottom view of SSORMM

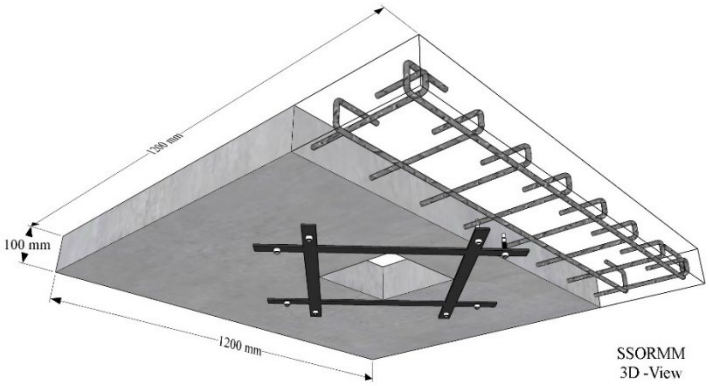

SSORMM
3D -View

e2. 3D view of SSORMM

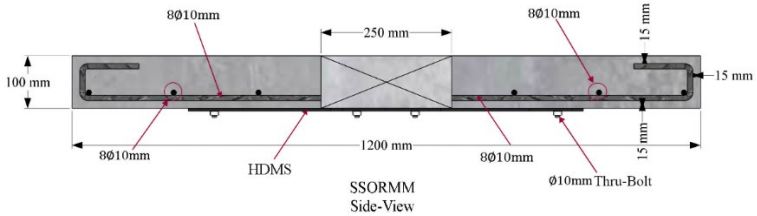

SSORMM
Side-View

e3. Section of SSORMM

e. Detail of the SSORMM specimen

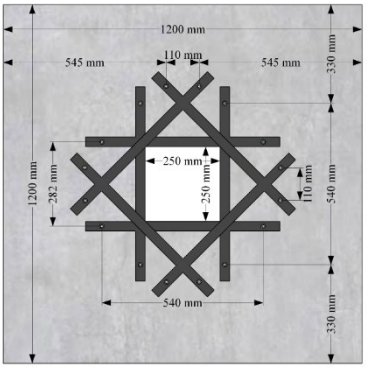

f1. Bottom view of SSO4RMM

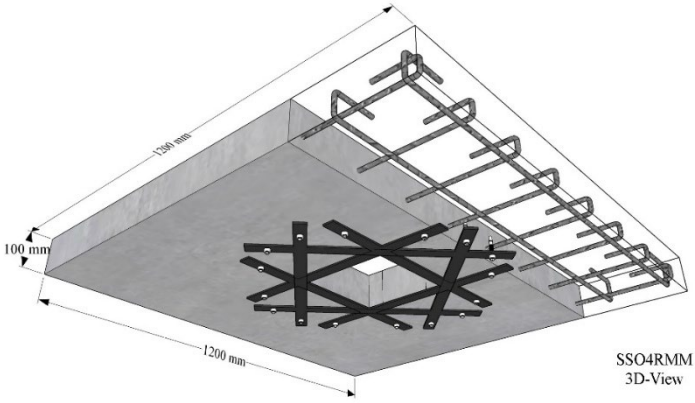

f2. 3D view of SSO4RMM

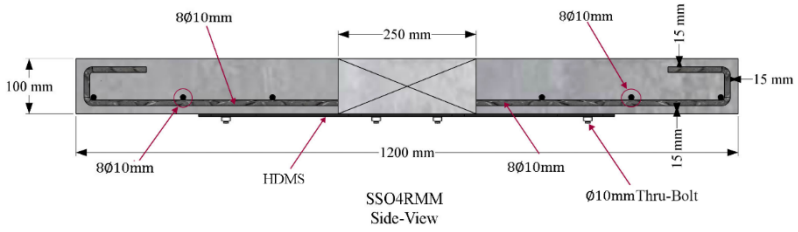

f3. Section of SSO4RMM

f. Detail of the SSO4RMM specimen

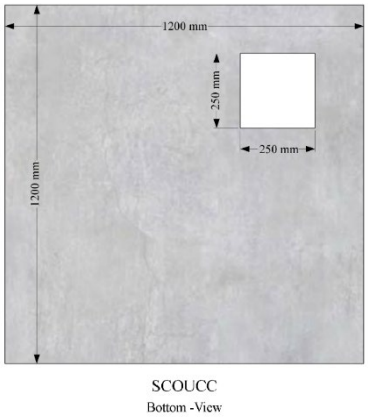

g1. Bottom view of SCOUCC

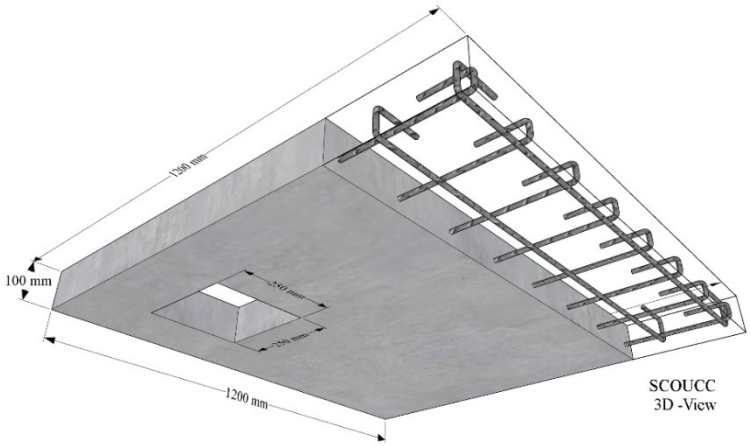

g2. 3D view of SCOUCC

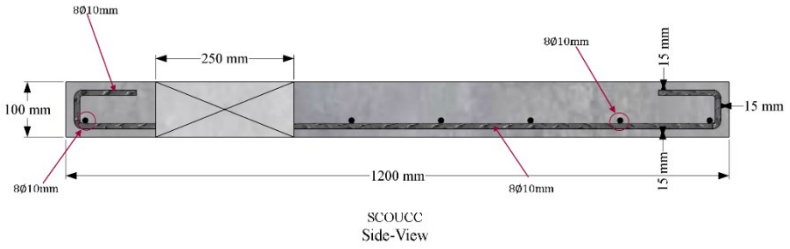

g3. Section of SCOUCC

g. Detail of the SCOUCC specimen

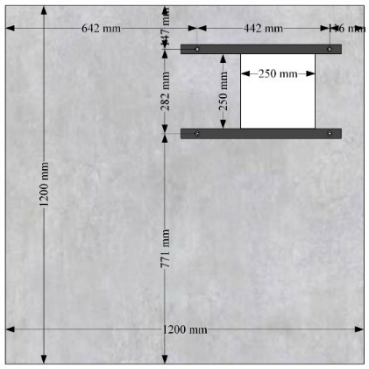

SSO2CC
Bottom - View

h1. Bottom view of SSO2CC

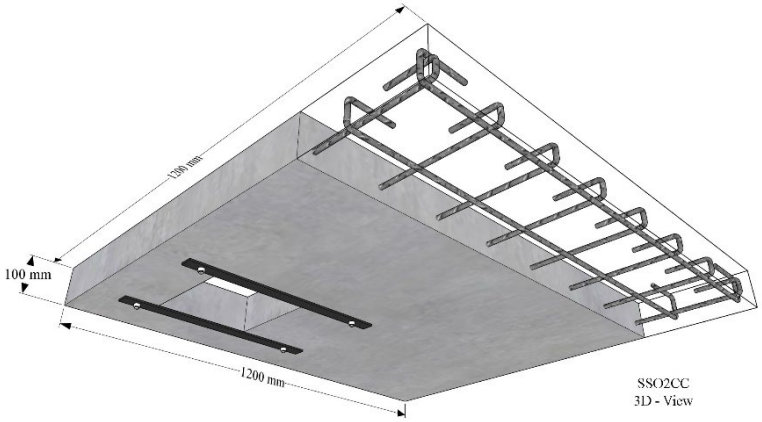

SSO2CC
3D - View

h2. 3D view of SSO2CC

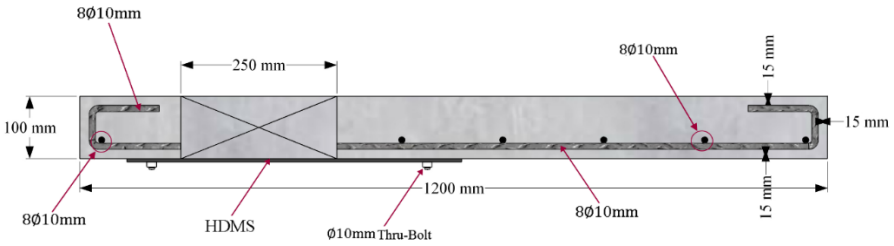

SSO2CC
Side-View

h3. Section of SSO2CC

h. Detail of the SSO2CC specimen

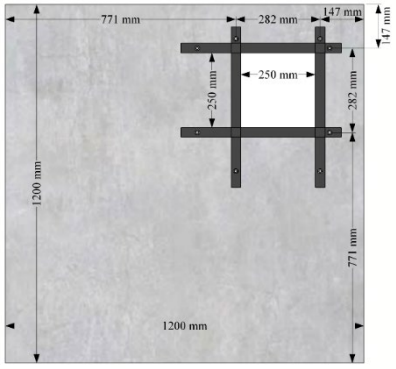

i1. Bottom view of SSO4CC

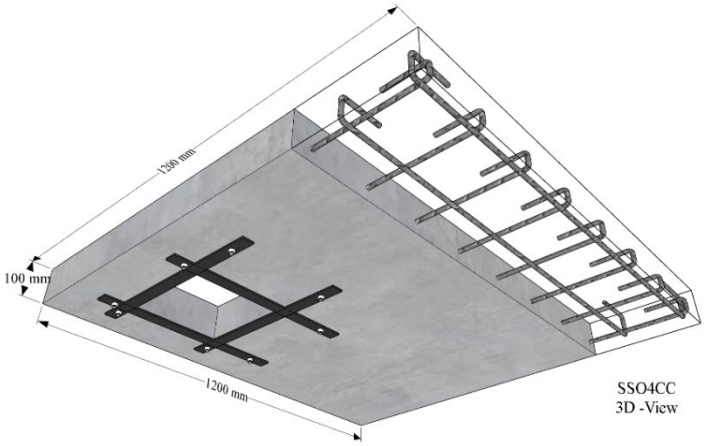

i2. 3D view of SSO4CC

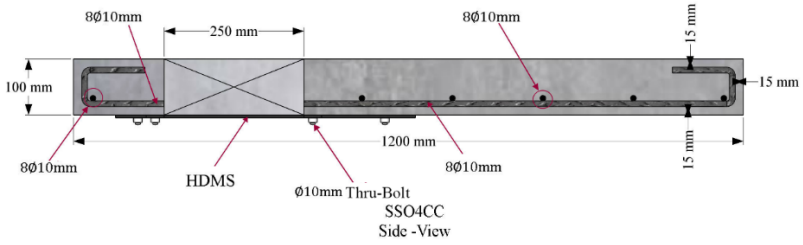

i3. Section of SSO4CC

i. Detail of the SSO4CC specimen

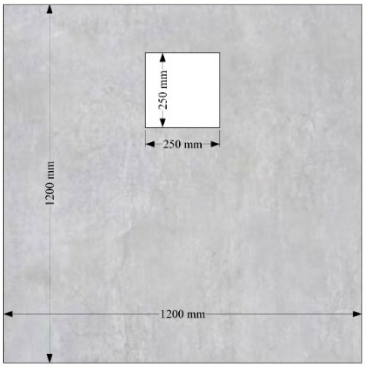

SCOUMC
Bottom -View

j1. Bottom view of SCOUMC

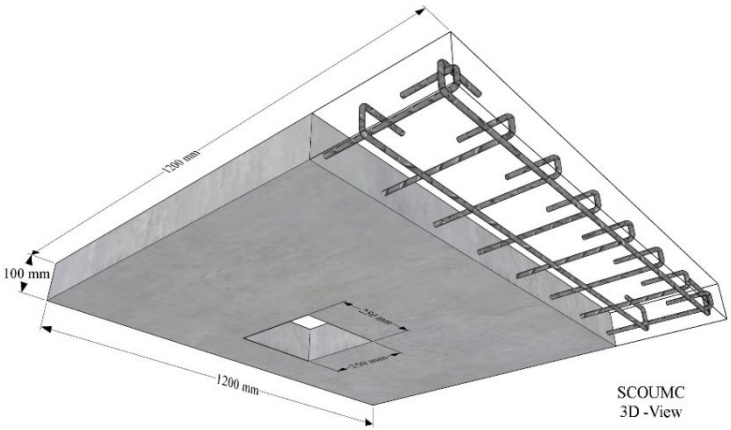

SCOUMC
3D -View

j2. 3D view of SCOUMC

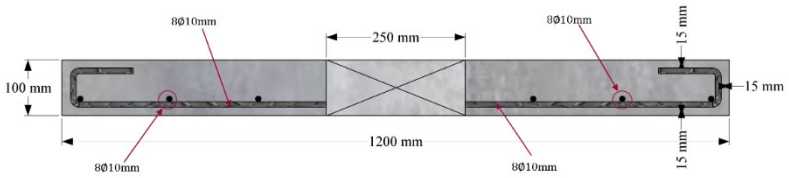

SCOUMC
Side-View

j3. Section of SCOUMC

j. Detail of the SCOUMC specimen

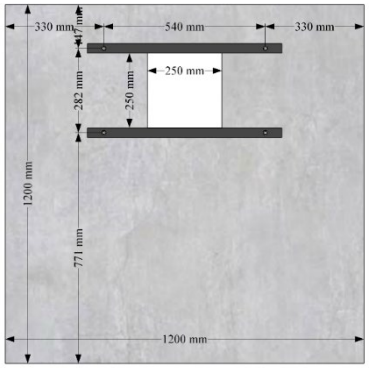

k1. Bottom view of SSO2MC

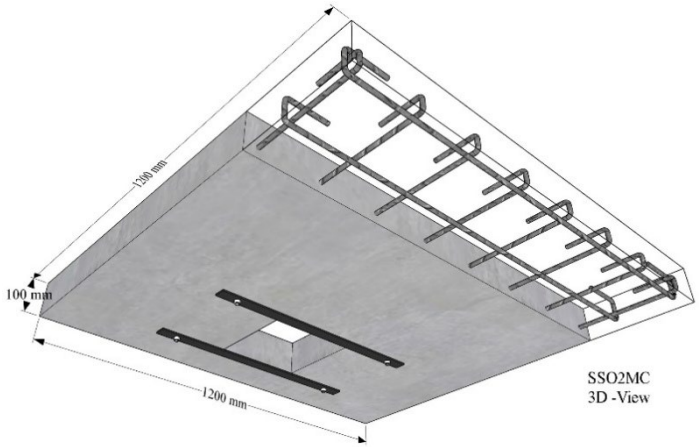

k2. 3D view of SSO2MC

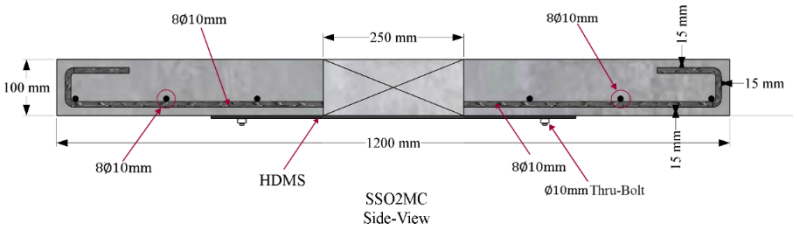

k3. Section of SSO2MC

k. Detail of the SSO2MC specimen

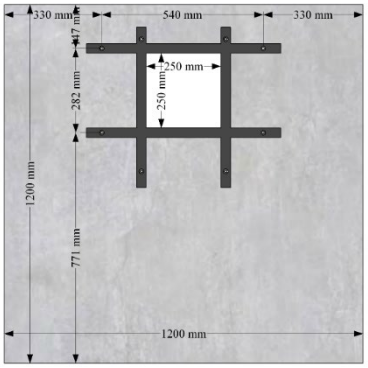

SSO4MC
Bottom -View

l1. Bottom view of SSO4MC

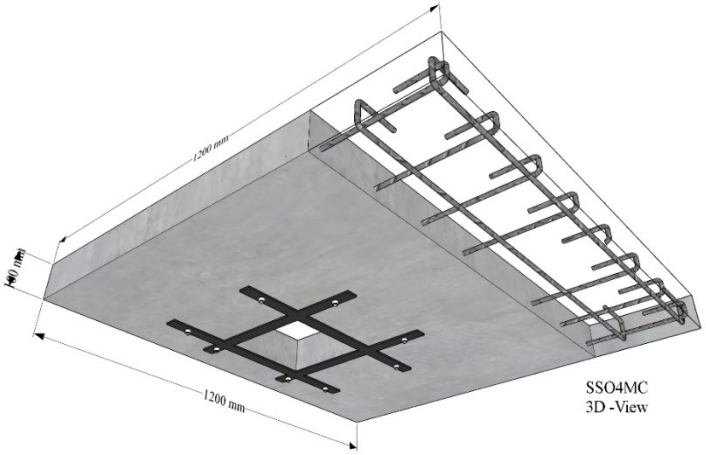

l2. 3D view of SSO4MC

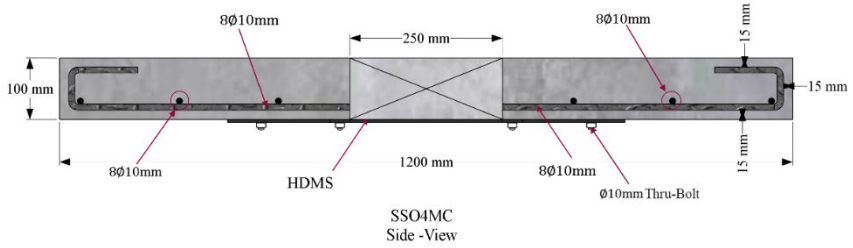

l3. Section of SSO4MC

l. Detail of the SSO4MC specimen

Figure 1. Detail of the tested specimens

Table 3. Concrete mix proportion

Material	Quantity
Cement (kg/m^3)	425
Coarse Aggregate (kg/m^3)	921
Fine Aggregate (kg/m^3)	1136
Water (kg/m^3)	205
w/c ratio	0.48

Figure 2. HDMS.

Table 4. Specifications of the metal straps

Batch	Dimensions (mm)	Surface	Tensile Strength (MPa)	Elongation (%)
E191015-1	32 x 0.8	BLACK PAINTED AND WAXED	935	9

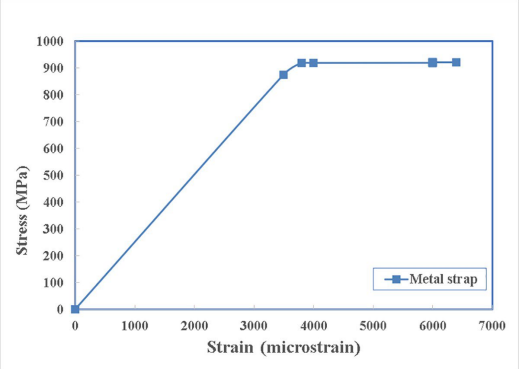

Figure 3. Load-Strain diagram of the HDMS.

Figure 4. Thru-Bolt

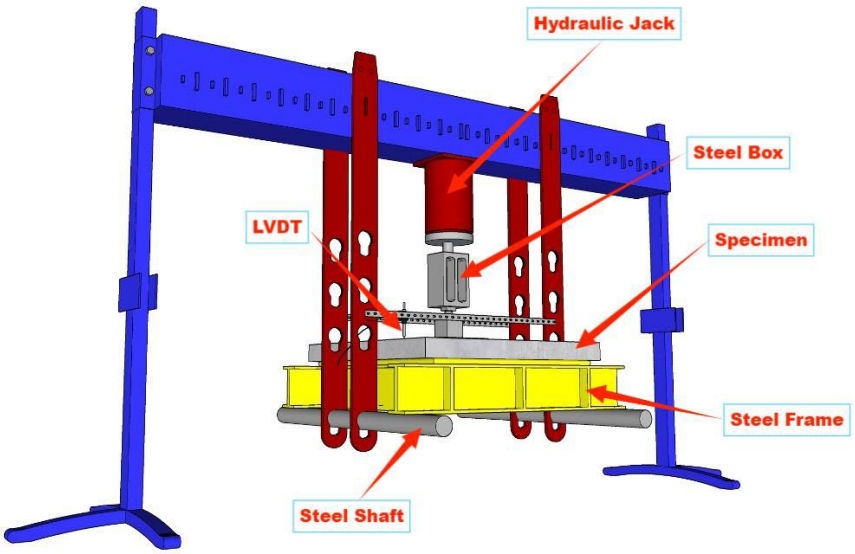

Figure 5. Test setup

Table 5. Test results

Groups	Specimen ID	P_{cr} (kN)	P_y (kN)	Δ_y (mm)	P_u (kN)	Δ_u(mm)	$P_u/P_{us\ control}$ (%)	DI (Δ_u/Δ_y)	Ky (kN/mm)	Ku (kN/mm)	Residual stiffness
Control	SCSU	34.60	135.71	6.85	180.95	10.41	100	1.52	19.81	12.71	7.10
I	SCOUMM	21.88	107.81	8.75	143.74	15.78	79	1.80	12.32	5.11	7.21
	SSO2MM	45.72	105.32	6.00	140.42	10.84	78	1.81	17.55	7.25	10.30
	SSO4MM	12.96	110.34	11.00	147.12	17.67	81	1.61	10.03	5.51	4.52
	SSORMM	20.00	108.90	10.68	145.20	16.86	80	1.58	10.20	5.87	4.32
	SSO4RMM	47.30	120.23	5.95	160.30	11.36	89	1.91	20.21	7.41	12.80
II	SCOUCC	12.20	130.50	8.60	174.00	14.26	96	1.66	15.17	7.69	7.49
	SSO2CC	17.00	131.85	8.50	175.80	17.30	97	2.04	15.51	4.99	10.52
	SSO4CC	35.60	126.08	6.70	168.10	13.60	93	2.03	18.82	6.09	12.73
III	SCOUMC	45.30	111.30	4.70	148.40	9.86	82	2.10	23.68	7.19	16.49
	SSO2MC	39.80	105.35	4.40	140.46	7.20	78	1.64	23.94	12.54	11.40
	SSO4MC	33.30	105.59	5.20	140.78	12.82	78	2.47	20.30	4.62	15.69

Note: P_{cr} = Cracking load in kN, P_u = Ultimate load in kN , Δ_u = Deflection at ultimate load in mm, P_y = Yield load in kN , Δ_y= Deflection at yield load in mm, DI= Ductility Index, K_y= Yield stiffness in kN/mm, $K_y = P_y/\Delta_y$, K_u= Ultimate stiffness in kN/mm, $K_u = (P_u - P_y) / (\Delta_u - \Delta_y)$.

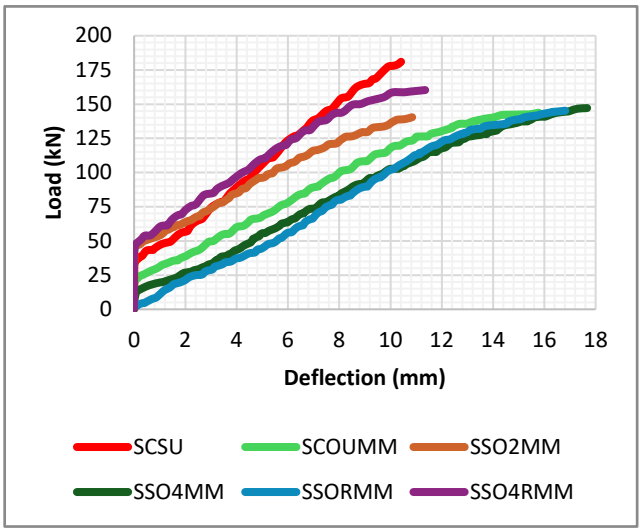

a-Load-Deflection diagram of group I

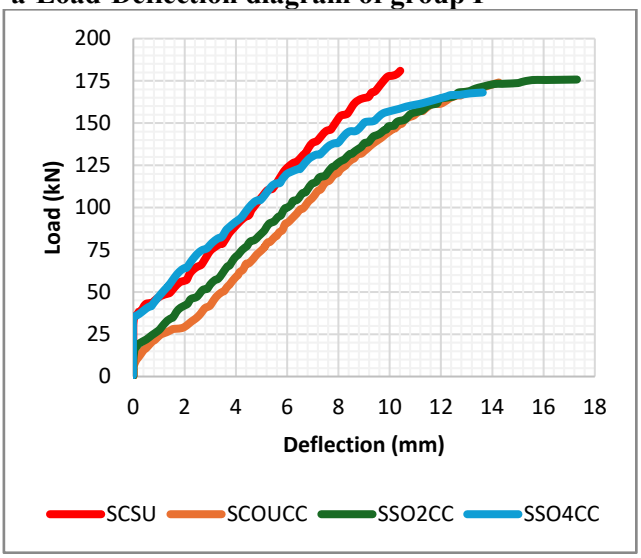

b-Load-Deflection diagram of group II

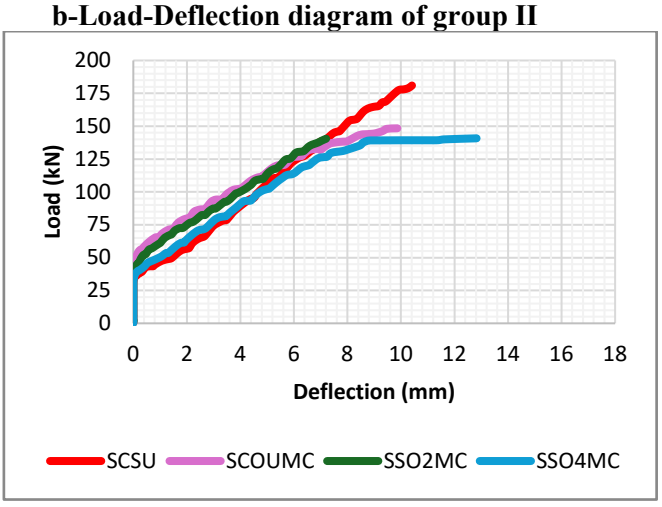

c-Load-Deflection diagram of group III

Figure 6. Load-Deflection diagram of the slabs

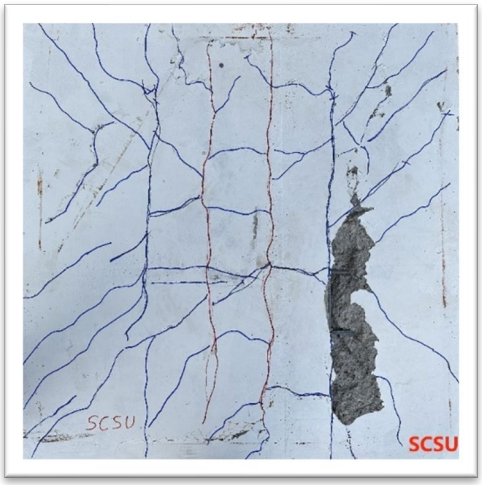

a. Bottom view of SCSU

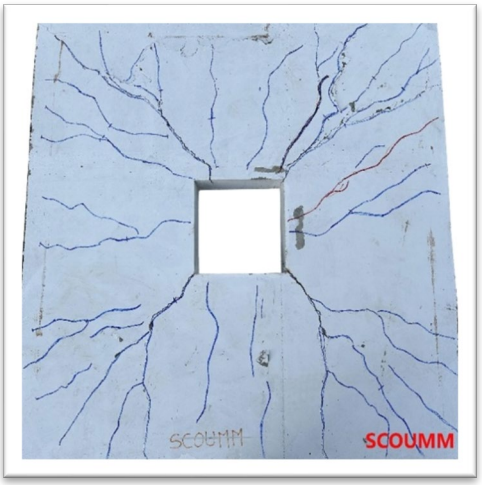

b. Bottom view of SCOUMM

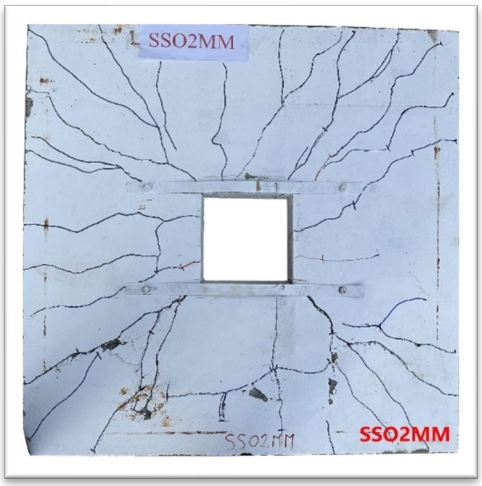

c. Bottom view of SSO2MM

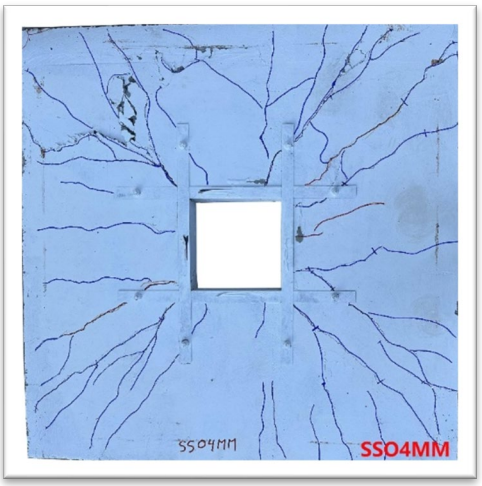

d. Bottom view of SSO4MM

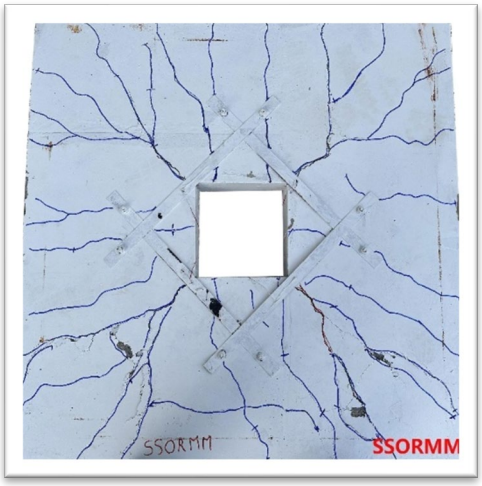

e. Bottom view of SSORMM

f. Bottom view of SSO4RMM

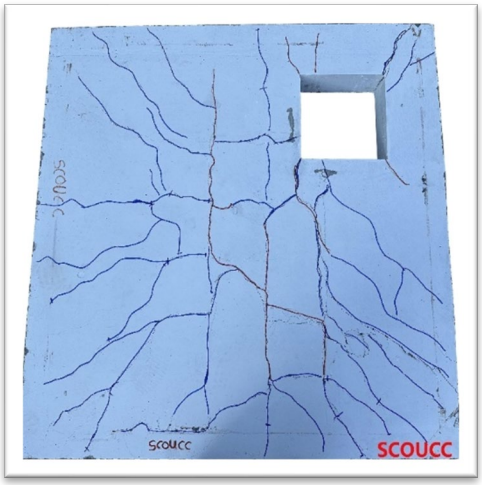

g. Bottom view of SCOUCC

h. Bottom view of SSO2CC

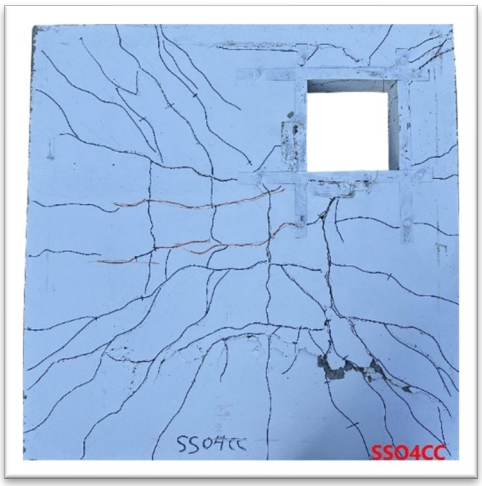

i. Bottom view of SSO4CC

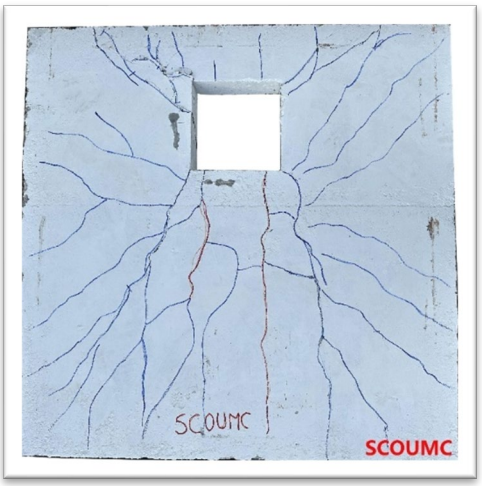

j. Bottom view of SCOUMC

k. Bottom view of SSO2MC

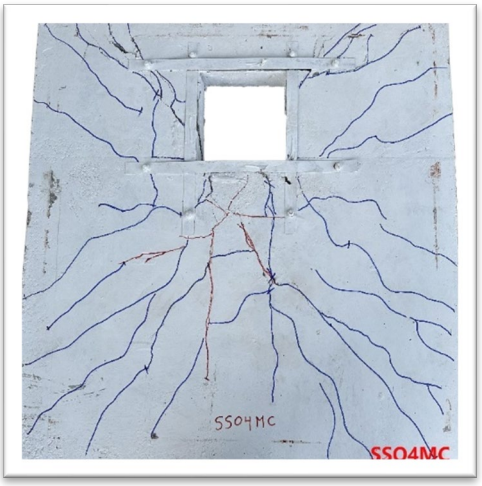

l. Bottom view of SSO4MC

Figure 7. Crack pattern on the tension face and the failure mode of the specimens